

# The X-Ray Population of NGC 300

S. Carpano<sup>1</sup>, J. Wilms<sup>2</sup>, E. Kendziorra<sup>1</sup> and M. Schirmer<sup>3</sup>

<sup>1</sup>Institut für Astronomie und Astrophysik, Abteilung Astronomie, Universität Tübingen, Sand 1, 72076 Tübingen, Germany  
email: stefania.carpano@uni-tuebingen.de

<sup>2</sup>Department of Physics, University of Warwick, Coventry, CV4 7AL, United Kingdom

<sup>3</sup>Isaac Newton Group of Telescopes, 38700 Santa Cruz de La Palma, Spain

**Abstract.** We present X-ray properties of NGC 300 point sources, extracted from 66 ksec of *XMM-Newton* data taken in 2000 December and 2001 January. A total of 163 sources was detected in the energy range of 0.3–6 keV. We report on the global properties of the sources detected inside the  $D_{25}$  optical disk, such as the hardness ratio and X-ray fluxes, and spectral fitting of the brightest sources. We also present some properties of their optical counterparts found in B, V, and R images from the 2.2 m MPG/ESO telescope. Furthermore, we cross-correlate the X-ray sources with SIMBAD, the USNO-A2.0 catalog, and radio catalogues.

**Keywords.** Galaxies: individual: NGC 300 – X-rays: galaxies.

---

## 1. Introduction

NGC 300 is a normal dwarf galaxy of type SA(s)d belonging to the Sculptor galaxy group. Due to its small distance ( $\sim 2.02$  Mpc; Freedman *et al.* 2001), its low Galactic column density ( $N_{\text{H}} = 3.6 \times 10^{20} \text{ cm}^{-2}$ ; Dickey & Lockman 1990) and its face-on orientation, this galaxy is an ideal target for the study of the entire X-ray population of a typical normal quiescent spiral galaxy. The major axes of the  $D_{25}$  optical disk are 13.3 kpc and 9.4 kpc ( $22' \times 15'$ ; de Vaucouleurs *et al.* 1991).

NGC 300 has already been observed by *ROSAT* five times between 1991 and 1997. Read & Pietsch (2001) discovered a total of 29 sources within the  $D_{25}$  disk, the brightest being a black hole candidate with  $L_{\text{X}} = 2.2 \times 10^{38} \text{ erg s}^{-1}$  in the 0.1–2.4 keV band. More recently, NGC 300 was observed with *XMM-Newton* on 2000 December 26 during *XMM-Newton*'s revolution 192 and 6 days later during revolution 195. The luminous supersoft X-ray source XMMU J005510.7–373855 in the center of NGC 300 has been analysed by Kong & Di Stefano (2003). In addition to these X-ray data, observations with the 2.2 m MPG/ESO telescope in La Silla were performed. We use archival images in the broad band B, V, and R filters for this work.

Here, we present some X-ray properties of NGC 300 point sources, extracted from 66 ksec of *XMM-Newton* data and spectral fitting of the brightest sources. Some previous results of these observations were presented by Kendziorra *et al.* (2001) and Carpano *et al.* (2004), a full description of our results can be found in Carpano *et al.* (2005).

## 2. Results

We reduced the data using the standard *XMM-Newton* Science Analysis System (SAS), version 6.1.0. Spectra, images, and lightcurves were extracted using `evselect`.

Event and attitude file of each instrument were first merged for both orbits 192 and 195 using the `merge` task. Point source detection was then performed on the three cameras using the maximum likelihood approach of the `edetect_chain` task. After removing

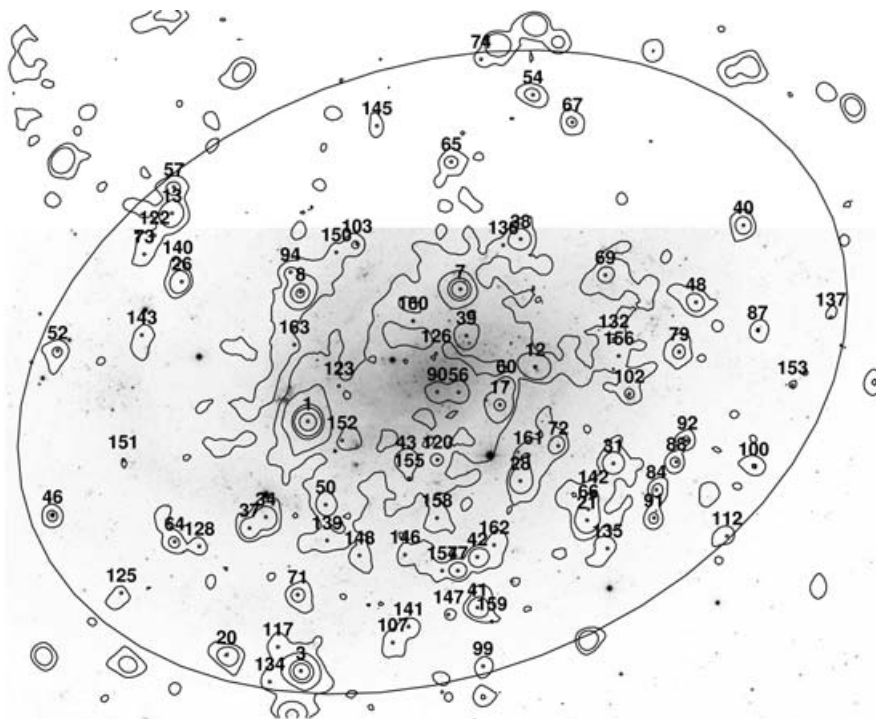


**Figure 1.** Optical image of NGC 300 in the visible band overlaid by a contour map of the merged 0.3–6.0 keV raw X-ray image from all three EPIC cameras and from both orbits. The  $D_{25}$  optical disk and the sources detected inside the disk are also shown.

sources associated with the galaxy cluster CL 0053–37, a total of 163 sources was found above a maximum likelihood threshold of 10 in the 0.3–6.0 keV band, 86 sources of which are within the  $D_{25}$  optical disk. This increases the X-ray inventory of NGC 300 by a factor of  $\sim 3$ .

Fig. 1 shows the V band optical image of NGC 300 and the contour map of the merged X-ray raw image from both orbits and all three EPIC cameras in the 0.3–6.0 keV energy band. The  $D_{25}$  optical disk and the sources detected inside the disk, which are numbered in order of decreasing X-ray count rate as determined by the `edetect_chain`, are also shown.

Our detection limit in the 0.3–6.0 keV energy band is  $F_{0.3-6} \sim 7 \times 10^{-16} \text{ erg cm}^{-2} \text{ s}^{-1}$  for sources inside the optical disk. We computed the hardness ratio of the X-ray sources using a soft, medium, and hard energy band of 0.3–1.0, 1.0–2.0, 2.0–6.0 keV respectively. Comparing the color-color diagram for sources inside the  $D_{25}$  optical disk and having more than 20 net counts, with empirical color-color diagrams, we were able to determine the shape of the X-ray spectrum for each source individually and to estimate source fluxes. These are between  $\sim 3.5 \times 10^{-13} \text{ erg cm}^{-2} \text{ s}^{-1}$  for the brightest one to  $\sim 7 \times 10^{-16} \text{ erg cm}^{-2} \text{ s}^{-1}$ .

After correcting the X-ray positions for the systematic shift between optical and X-ray coordinates, we searched for all possible optical counterparts in the merged BVR optical image and then calculate their fluxes in each of these three optical bands. Results are tabulated in Carpano *et al.* (2005). For the four brightest X-ray sources within the  $D_{25}$  ellipse, Fig. 2 shows the resulting optical counterparts in the merged optical image. Furthermore, we cross-correlated the X-ray sources with SIMBAD, the USNO-A2.0 catalog, and radio catalogues: 14 of our X-ray sources detected inside the optical disk have already

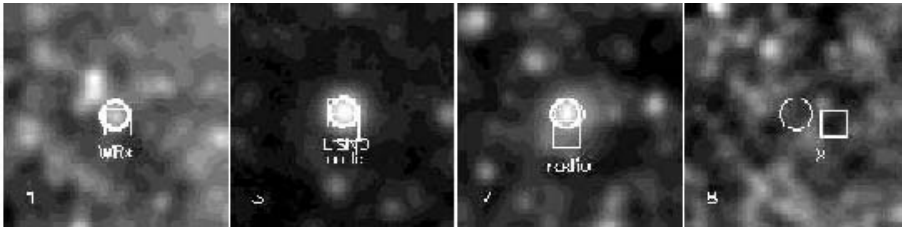


**Figure 2.** 15'' × 15'' optical images of the region centered on the corrected position of the four brightest X-ray sources inside the  $D_{25}$  optical disk. The circle indicates the  $2\sigma$  positional error of the X-ray coordinates, the thicker circles show the optical sources found within the X-ray error circle. Catalog sources having a distance of less than 5'' from the X-ray position are shown with a box.

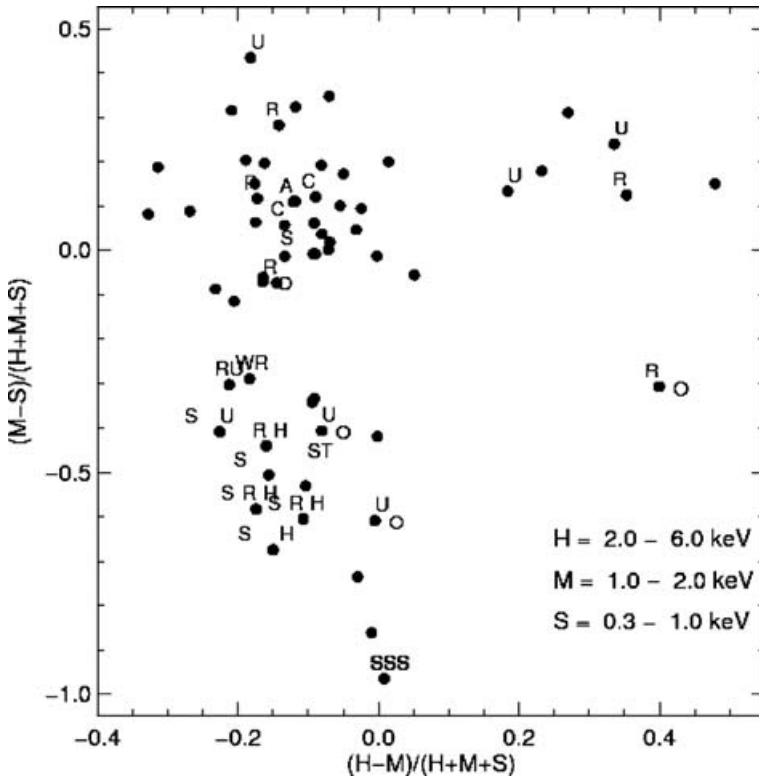


**Figure 3.** Color-color diagram for sources inside the optical disk. SNR are labeled with a ‘S’, radio sources with a ‘R’, H II regions with an ‘H’, Cepheid stars with a ‘C’, associations of stars with an ‘A’, stars in NGC 300 with a ‘ST’, Wolf-Rayet stars with a ‘WR’ and sources from the USNO catalog with a ‘U’. ‘SSS’ refers to the supersoft source and ‘O’ are possible foreground stars.

been observed in the X-rays, there are 9 (suspected) Supernova Remnants (SNRs), 11 radio sources, from which 3 are associated with SNRs and 8 are possible AGNs. Other sources are matching with an association of stars, with H II (ionized) regions, with regions close to Cepheid variable stars, or with stars.

Fig. 3 shows the color-color diagram for the sources detected inside the optical disk and, when available, a label indicating the counterparts found in SIMBAD, USNO and radio catalogs. Following Pietsch *et al.* (2004) and Pietsch *et al.* (2005), soft sources with  $\log(F_X/F_{\text{vis}}) = \log(F_X) + m_V/2.5 + 5.37 < -1$ , where  $m_V$  is the visual magnitude, are identified with foreground stars.

**Table 1.** Best fit parameters for the four brightest sources.

source label	model	$N_{\text{H}}(\times 10^{22} \text{ cm}^2)$	T (keV)	$\Gamma$	$\chi^2$	dof	$\chi^2_{\nu}$
1 (revol. 192)	power+brems	$0.08^{+0.05}_{-0.04}$	$0.28^{+0.04}_{-0.06}$	$1.78^{+0.23}_{-0.23}$	566.53	495	1.14
(revol. 195)		$0.10^{+0.03}_{-0.02}$	$0.43^{+0.11}_{-0.12}$	$2.25^{+0.20}_{-0.19}$			
3	power+brems	$0.18^{+0.03}_{-0.07}$	$0.28^{+0.15}_{-0.06}$	$2.24^{+0.34}_{-0.45}$	125.82	116	1.08
7	power	$0.35^{+0.05}_{-0.03}$		$1.91^{+0.12}_{-0.13}$	154.64	110	1.41
8	tbody	$0.11^{+0.04}_{-0.04}$	$0.061^{+0.004}_{-0.003}$		73.29	53	1.38

**Table 2.** 0.3–2.4 keV source luminosity in units of  $\times 10^{38} \text{ erg s}^{-1}$  of the four brightest sources.

source label	revol. 192	revol. 195	ROSAT ( $L_{0.1-2.4} \text{ keV}$ )
1 (pn)	$0.79^{+0.10}_{-0.11}$	$1.74^{+0.24}_{-0.49}$	$2.06 \pm 0.07$
3 (pn)	$0.35^{+0.06}_{-0.07}$	$0.45^{+0.06}_{-0.06}$	$0.64 \pm 0.04$
7 (pn)	$0.28^{+0.02}_{-0.02}$	$0.21^{+0.01}_{-0.01}$	$0.12 \pm 0.02$
8 (MOS1)	$0.44^{+0.13}_{-0.13}$	$0.22^{+0.04}_{-0.04}$	$0.48 \pm 0.04$

Except for one source, all SNR are located in a same region of the color-color diagram. The brightest source, having the WR star as optical counterpart, and which is a good candidate for a black hole X-ray binary, is slightly above the SNR group. The SSS is at the very bottom of the diagram and all harder sources, mainly hard X-ray binaries and background AGN, are spread on a large region in the upper part of the diagram.

We also performed spectral fitting for the four brightest X-ray sources inside the  $D_{25}$  optical disk. Results of the best spectral fits are shown in Table 1.

Fits were performed using data from the pn, MOS1, and MOS2, and both revolutions. The brightest source is the only one for which the hardness ratio has changed significantly between the two observations. Except for this source, we constrain the parameters of the spectral fitting to be equal for both revolutions.

For each of the sources, the pn (MOS1 for source 8) 0.3–2.4 keV luminosities are tabulated (Table 2) and compared to the value given by ROSAT (Read & Pietsch 2001), after that their luminosities have been recalculated considering a distance to NGC 300 of 2.02 Mpc (Freedman *et al.* 2001). All sources seem to be variable and are candidates for X-ray binaries.

## References

- Carpano, S., Wilms, J., Schirmer, M., & Kendziorra, E. 2004, *Mem. Soc. Astron. Italiana*, 75, 486
- Carpano, S., Wilms, J., Schirmer, M., & Kendziorra, E. 2005, *A&A*, accepted
- de Vaucouleurs, G., de Vaucouleurs, A., Corwin, jr., H., *et al.* 1991, *Third Catalogue of Bright Galaxies* (New York: Springer)
- Dickey, J. M. & Lockman, F. J. 1990, *ARA&A*, 28, 215
- Freedman, W. L., Madore, B. F., Gibson, B. K., *et al.* 2001, *ApJ*, 553, 47
- Kendziorra, E., Wilms, J., Lamer, G., & Staubert, R. 2001, in *New Visions of the X-ray Universe in the XMM-Newton and Chandra Era*, ed. F. Jansen *et al.*, ESA SP-488, ESA Publications, Noordwijk, in press
- Kong, A. K. H. & Di Stefano, R. 2003, *ApJ*, 590, L13
- Pietsch, W., Misanovic, Z., Haberl, F., Hatzidimitriou, D., Ehle, M., & Trinchieri, G. 2004, *A&A*, 426, 11
- Pietsch, W., Freyberg, M., & Haberl, F. 2005, *A&A*, 434, 483
- Read, A. M. & Pietsch, W. 2001, *A&A*, 373, 473